Orientation effects on the bandgap and dispersion behavior of $0.91Pb(Zn_{1/3}Nb_{2/3})O_3$–$0.09PbTiO_3$ single crystals*

He Chong-Jun(赫崇君)†, Fu Xin-Duo(付信夺), Xu Feng(徐 峰), Wang Ji-Ming(王吉明), Zhu Kong-Jun(朱孔军), Du Chao-Ling(杜朝玲), and Liu You-Wen(刘友文)‡

Nanjing University of Aeronautics and Astronautics, Nanjing 210016*, China*

(Received 21 July 2011; revised manuscript received 22 September 2011)

$0.91Pb(Zn_{1/3}Nb_{2/3})O_3$–$0.09PbTiO_3$ (PZN–9%PT) single crystals with different orientations are investigated by using a spectroscopic ellipsometer, and the refractive indices and the extinction coefficients are obtained. The Sellmeier dispersion equations for the refractive indices are obtained by the least square fitting, which can be used to calculate the refractive indices in a low absorption wavelength range. Average Sellmeier oscillator parameters E_o, λ_o, S_o, and E_d are calculated by fitting with the single-term oscillator equation, which are related directly to the electronic energy band structure. The optical energy bandgaps are obtained from the absorption coefficient spectra. Our results show that the optical properties of [001] and [111] poled crystals are very similar, but quite different from those of the [011] poled crystal.

Keywords: dispersion, bandgap, orientation

PACS: 42.50.Ct, 78.20.Ci, 78.20.–e **DOI:** 10.1088/1674-1056/21/5/054207

1. Introduction

Single crystals of relaxor rhombohedral $(1-x)Pb(Zn_{1/3}Nb_{2/3})O_3$–$xPbTiO_3$ (PZN–xPT, $0 < x < 0.1$) cut and poled in the [001] direction exhibit extraordinarily large dielectric and piezoelectric constants,[1−5] and have been used for electromechanical transducers and actuators in a broad range of advanced applications, such as medical ultrasonic imaging and underwater communication.[6−9] Materials with large piezoelectric effects often have large electro-optic effects too, because the combination of the piezoelectric and the photoelastic effects substantially enhances the electro-optic effect. A large electro-optic effect has been observed in PZN–xPT single crystals with compositions near the morphotropic phase boundary (MPB).[10−14] For PZN–8%PT single crystal poled along the $\langle 001 \rangle$ direction, $\gamma_{33} \sim 450$ pm/V, for PZN–10%PT single crystal, $\gamma_{33} \sim 177$ pm/V ($\lambda = 632.8$ nm).[15,16] Therefore, PZN–xPT single crystals could be good candidates for use in highly efficient electro-optic devices.

In spite of the intensive research on the large piezoelectric response, the optical properties of PZN–xPT single crystals have not been sufficiently understood. Optical dispersion plays an important role in the research of optical materials, because it is a significant factor in designing devices of spectral dispersion and optical communication. The optical bandgaps of the ferroelectric crystals are of great interest for theoretical studies and numerous applications in quantum optics. In the present work, the optical properties of PZN–9%PT single crystals with different orientations are investigated. The dispersions of the refractive indices are described in terms of the Sellmeier dispersion equations, and the optical bandgaps are estimated after the extinction coefficient spectra have been obtained.[17]

*Project supported by the National Natural Science Foundation of China (Grant Nos. 60808026, 11174147, 50872053, 50902027 and 11004103), the Specialized Research Fund for the Doctoral Program of Higher Education, China (Grant No. 20093218120030), the Nanjing University of Aeronautics and Astronautics Research Funding, China (Grant No. NP2011037), the Program for New Century Excellent Talents in University, China (Grant No. NCET-10-0070), the Prior Project in Key Science & Technology Program of Zhejiang Province, China (Grant No. 2009C11144), and the Cultivation Fund of the Key Scientific and Technical Innovation Project of Ministry of Education of China (Grant No. 707031).

†Corresponding author. E-mail: hechongjun@nuaa.edu.cn

‡Corresponding author. E-mail: ywliu@nuaa.edu.cn

© 2012 Chinese Physical Society and IOP Publishing Ltd

2. Experiment

High-quality and large-size PZN–9%PT single crystals were grown by using a modified Bridgman technique.[18,19] The unpoled ferroelectric crystals were macroscopically of the $m3m$ phase. Namely, each of them retained an optical isotropic pseudocubic state. The grown crystals were oriented along the [001], the [011], or the [111] direction using an X-ray orientation device and an X-ray diffractometer. Then the crystals were cut into square slices. Silver paste was painted on the sample surfaces and sintered at 580 °C for 30 min. The samples were poled under an electric field of 1 kV/mm for 15 min near 150 °C in silicone oil, then slowly cooled to room temperature while maintaining half of the applied electric field.

The square surfaces for light reflection were mirror-polished using alumina and diamond polishing compounds (with decreasing average grit size down to 0.25 μm). The spectroscopic ellipsometer is a very powerful technique to measure the refractive index and the extinction coefficient. Optical measurements were carried out at room temperature by using a spectroscopic phase-modulated ellipsometer (Jobin YVON UVISEL). An incidence angle of 70° and intervals of 1.6 nm were used throughout our measurements.

3. Results and discussion

3.1. Refractive index and extinction coefficient

In the spectroscopic ellipsometer, a linearly polarized monochromatic light illuminates the sample surface, relative changes in amplitude and phase of the reflected light are measured. Generally, the spectroscopic ellipsometer measures the traditional ellipsometric angles each as a function of the wavelength. They are related to optical and structural properties of the samples as

$$\rho = \tan\Psi\, \mathrm{e}^{\mathrm{i}\Delta} = \frac{R_\mathrm{p}}{R_\mathrm{s}} = \left|\frac{R_\mathrm{p}}{R_\mathrm{s}}\right| \exp[\mathrm{i}(\delta_\mathrm{p} - \delta_\mathrm{s})], \qquad (1)$$

where the complex Fresnel reflection coefficients R_p and R_s correspond to the parallel and the perpendicular components, respectively. They are complex functions of refractive index n and extinction coefficient k. For the bulk isotropic samples investigated here, their complex refractive indexes ($\tilde{n} = n + \mathrm{i}k$) can be revealed automatically by comparing the computer modeling data with the experimental data.

Figure 1 shows refractive index n and extinction coefficient k of PZN–9%PT crystals each as a function of the wavelength for different orientations. In general, the refractive indexes appear to continuously decrease nonlinearly with the increase of the wavelength over the entire range of wavelength. However, the extinction coefficients decrease more sensitively at lower wavelengths and are flat at wavelengths above 500 nm. This behavior is typical for an insulator or a semiconductor in the range of wavelength near the bandgap. Below the bandgap, the transmission dominates with a tiny extinction coefficient. This indicates that PZN–9%PT single crystals are transparent in the visible light region, which is consistent with the results obtained in their optical transmission spectra.[12,20] For PZN–xPT single crystals, the main contribution of optical loss comes from the bandgap as well as the domain wall scattering. These mechanisms become increasingly important when the photon energies are near the bandgap.

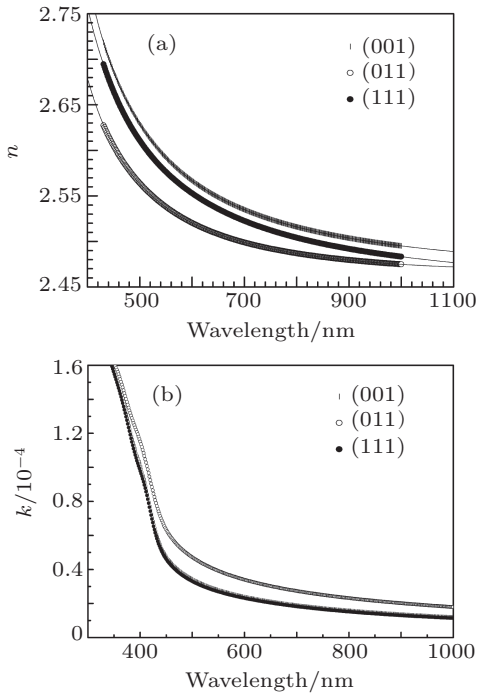


Fig. 1. (a) Refractive indexes and (b) extinction coefficients of PZN–9%PT single crystals with different orientations each as a function of wavelength. Solid curves in panel (a) are the fitting results with dispersion Eq. (2).

3.2. Dispersion behavior

The typical Sellmeier dispersion equation of crystal is

$$n^2 = A + \frac{B}{\lambda^2 - C} - D\lambda^2, \qquad (2)$$

where A, B, C, and D are all constants, and λ is the wavelength in micrometers. These constants are shown in Table 1, which are obtained by the least square fitting of Eq. (2).[21] The dispersion behaviors of PZN–9%PT single crystals are similar to

those of most ABO_3 type perovskite structure compounds, since they are all oxygen-octahedron ferroelectrics. The basic BO_6 octahedron building block in perovskite ferroelectrics leads to the similarities in the band structure and in the polarization-induced Stark-like energy band shifts. The B-cation d orbitals and the O-anion 2p orbitals associated with each octahedron are the major contributors to the refractive indexes. The common structural unit in oxygen-octahedron ferroelectrics leads to the similar dispersion behavior.[22]

Table 1. Coefficients in the Sellmeier dispersion equation for PZN–9%PT single crystals with different orientations.

Orientation	[001]	[011]	[111]
A	6.071(5)	5.991(7)	6.031(9)
B	0.149(2)	0.101(6)	0.144(9)
C	0.072(1)	0.075(5)	0.069(5)
D	0.006(3)	–0.026(9)	0.018(8)

Equation (2) fits the dispersion of refractive index quite well for most materials. However, the resulting curve fitting parameters have no special physical significance. By using an excellent long-wavelength approximation, Wemple and Didomenico[23] developed a single-term Sellmeier relation

$$n^2 - 1 = \frac{S_o \lambda_o^2}{1 - \lambda_o^2/\lambda^2} = \frac{E_d E_o}{E_o^2 - E^2}, \tag{3}$$

where n is the refractive index, S_o is the average oscillator strength, λ_o is the average oscillator position, E_o is the single oscillator energy, E_d is the dispersion energy, λ and E are the wavelength and the energy of the incident light, respectively. The parameters in Eq. (3) can be obtained by plotting $1/(n^2-1)$ versus λ^{-2} and E^2 as shown in Fig. 2. The results are listed in Table 2. The refractive index dispersion parameter E_o/S_o describes the dispersion behavior, depends on the characteristics of the interband transitions, and enters directly into the evaluation of the electro-optic and nonlinear optical constants of the oxygen-octahedron ferroelectrics.

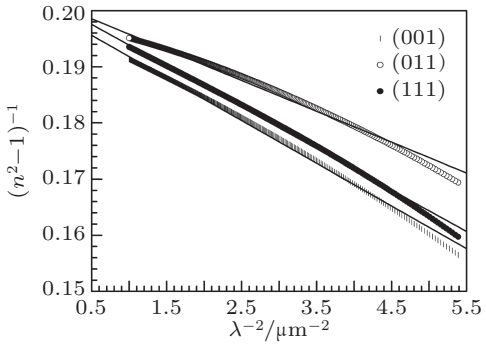


Fig. 2. Linear fitting curves of λ^{-2} dependence of $(n^2-1)^{-1}$ for PZN–9%PT single crystals with different orientations.

Table 2. Single oscillator dispersion parameters, bandgap E_g, and Urbach energy E_U of PZN–9%PT single crystals with different orientations.

Orientation	[001]	[011]	[111]
E_o/eV	6.352(8)	7.506(16)	6.477(6)
E_d/eV	31.85(4)	37.29(8)	32.19(3)
λ_o/μm	0.1952(2)	0.1652(4)	0.1914(2)
$S_o/10^{14}$ m^{-2}	1.316(3)	1.820(9)	1.356(3)
$E_o \cdot S_o^{-1}/10^{-14}$ eV·m^2	4.827(6)	4.124(9)	4.777(5)
E_g/eV	3.04(3)	2.98(7)	3.09(8)
E_U/eV	0.442(6)	0.530(5)	0.446(6)

3.3. Bandgap

The dominating features in the optical properties of PZN–xPT for wavelengths above 400 nm come from the interband electronic transitions between the low-lying conduction bands and the upper valence bands. It is, therefore, useful to investigate the change in the bandgap as the crystal orientation changes. In order to determine the bandgap energy, the absorption coefficient α of the single crystal is derived from the extinction coefficients k as

$$\alpha = 4\pi k/\lambda. \tag{4}$$

The bandgap of PZN–9%PT single crystal can be deduced from absorption coefficient α through the Tauc equation

$$\alpha h\nu = C(h\nu - E_g)^n, \tag{5}$$

where C is a constant, E_g is the allowed bandgap energy, $h\nu$ is the energy of the incident light, and n is the index determined by the nature of the electron transition in the absorption process.[24–26] It is well known that there are two types of fundamental optical transitions, namely direct transition and indirect transition ($n = 1/2$ for the allowed direct transition, $n = 2$ for the allowed indirect transition). As shown in Fig. 3, the curves of $(\alpha h\nu)^2$ versus $h\nu$ are found to change into straight lines near the absorption edge, thus supporting the interpretation of the direct rather than the indirect bandgap for all crystals. The straight lines of $(\alpha h\nu)^2$ versus $h\nu$ can be used to provide the values of optical bandgap E_g, which are extrapolated by the linear portions of the plots to $(\alpha h\nu)^2 = 0$. The bandgaps are listed in Table 2.

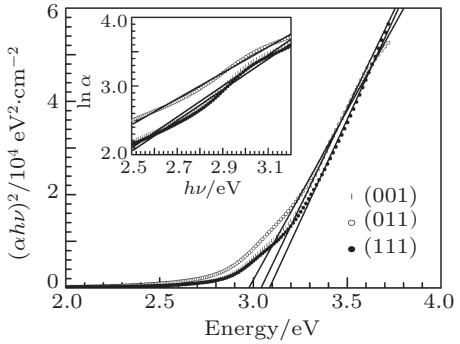


Fig. 3. Photon energy $h\nu$ dependences of $(\alpha h\nu)^2$ for PZN–9%PT single crystals with different orientations. The inset shows the linear fitting curves for obtaining the Urbach energy $E_{\rm U}$.

The absorption tail at lower photon energy usually follows the Urbach rule

$$\alpha = \alpha_0 \exp(h\nu/E_{\rm U}), \tag{6}$$

where α_0 is a constant, and $E_{\rm U}$ is the Urbach energy, which is interpreted as the width of the tail to the localized states in the bandgap.[27–29] The absorption in this region is due to the transitions between the extended states in one band and the localized states in the exponential tail of the other band. By plotting $\ln\alpha$ as a function of energy $h\nu$ in Fig. 3, the values of $E_{\rm U}$ can be obtained. As listed in Table 2, the Urbach energies of [001] and [111] oriented crystals are nearly the same, but lower than that of the [011] oriented crystal.

At room temperature, the PZN–9%PT single crystal has a rhombohedral phase ($3m$ symmetry). The $\langle 111\rangle$ is the spontaneous polar direction. After the crystal is poled along [111], its major phase is rhombohedral. The [001] poled crystal has an engineered multi-domain structure. The coexistence of domains with four equivalent polar vectors results in a 4-fold axis along [001], consequently resulting in the macroscopic symmetry $4mm$ from the local $3m$ symmetry.[30] After being poled along the [011] direction, which is the polar direction of the orthorhombic phase,[31] the metastable single domain state is induced.[32] For [111] and [001] poled PZN–9%PT crystals, the common microscopic structure results in a similar electronic energy band. Thus, they have similar optical behaviors, which are quite different from the [011] poled crystal.

4. Conclusion

Refractive indexes and extinction coefficients of PZN–9%PT single crystals with different orientations are measured by using a spectroscopic ellipsometer. The Sellmeier dispersion equations are obtained by means of least square fittings. The typical Sellmeier dispersion equation, which involves four parameters, is intrinsically capable of numerically fitting the dispersion of the refractive index to a higher accuracy than the single-oscillator Sellmeier equation that involves only two parameters. However, the single-oscillator Sellmeier equation is also important, because the oscillator parameters are of physical significance, which are related directly to the energy band structure. Our results show that the optical properties of [001] and [111] poled crystals are almost the same, but quite different from those of the [011] poled one. These results provide an important basis for further theoretical study and practical device fabrication of PZN–xPT single crystals.

Acknowledgment

Authors thank Professor Luo Hao-Su at the Shanghai Institute of Ceramics, Chinese Academy of Sciences, for providing the seed crystal and help in the crystal growth.

References

[1] Jin J, Rajan K K and Lim L C 2007 *IEEE Trans. Ultrason. Ferroelectr. Freq. Control* **54** 2222

[2] Delaunay T, Clezio E L, Guennou M, Dammak H, Thi M P and Feuillard G 2008 *IEEE Trans. Ultrason. Ferroelectr. Freq. Control* **55** 476

[3] Okawara1 C and Amin A 2009 *Appl. Phys. Lett.* **95** 072902

[4] Singh B K, Kumar K, Sinha N and Kumar B 2009 *Cryst. Res. Technol.* **44** 9150

[5] He C J, Jing W P, Wang F F, Zhu K J and Qiu J H 2011 *IEEE Trans. Ultrason. Ferroelectr. Freq. Control* **58** 1127

[6] Zhou D, Chen J, Luo L H, Zhao X Y and Luo H S 2008 *Appl. Phys. Lett.* **93** 073502

[7] Amin A, McLaughlin E, Robinson H and Ewart L 2007 *IEEE Trans. Ultrason. Ferroelectr. Freq. Control* **54** 1090

[8] Wang F F, Shi W Z and Luo H S 2010 *Rev. Sci. Instrum.* **81** 043904

[9] Moon K S, Levy M, Hong Y K and Park H K 2005 *IEEE Trans. Ultrason. Ferroelectr. Freq. Control* **52** 953

[10] Guo R, Liu H, Reyes G, Jamieson W and Bhalla A 2008 *Proc. SPIE* **7056** 705616

[11] Sato Y, Abe S, Fujimura R, Ono H, Oda K, Shimura T and Kuroda K 2004 *J. Appl. Phys.* **96** 4852

[12] Abe S, Fujishima T, Tsubone T, Fujimura R, Ono H, Matoba S, Oda K, Shimura T and Kuroda K 2003 *Opt. Lett.* **28** 420

[13] Bing Y, Guo R, Bhalla A and Josephkumar F 2000 *Ferroelectric Lett.* **30** 69

[14] Lu Y, Cheng Z Y, Park S E, Liu S F and Zhang Q 2000 *Jpn. J. Appl. Phys.* **39** 141

[15] Barad Y, Lu Y, Cheng Z Y, Park S E and Zhang Q M 2000 *Appl. Phys. Lett.* **77** 1247
[16] Lu Y, Cheng Z Y, Barad Y and Zhang Q M 2001 *J. Appl. Phys.* **89** 5075
[17] Gu C, Qu S B, Pei Z B and Xu Z 2011 *Chin. Phys.* B **20** 037801
[18] Xu J, Wu X, Tong J, Shi M and Qian G 2005 *J. Crystal Growth* **280** 107
[19] Jin M, Xu J, Shi M, Wu X and Tong J 2007 *Ultrason.* **2** 129
[20] Sun E, Zhang R, Wang Z, Xu D, Li L and Cao W 2010 *J. Appl. Phys.* **107** 113532
[21] Lv B, Zhou X, Linghu R F ,Wang X L and Yang X D 2011 *Chin. Phys.* B **20** 036104
[22] DiDomenico Jr M and Wemple S H 1969 *J. Appl. Phys.* **40** 720
[23] Wemple S H and Didomenico Jr M 1969 *Phys. Rev. Lett.* **23** 1156
[24] Zeng L G, Liu F M, Zhong W W, Ding P, Cai L G and Zhou C C 2011 *Acta Phys. Sin.* **60** 038203 (in Chinese)
[25] Di G Q 2011 *Acta Phys. Sin.* **60** 038101 (in Chinese)
[26] Liu M M and Ma X G 2011 *Chin. Phys.* B **20** 067801
[27] Ma X F, Wang Y Z and Zhou C Y 2011 *Acta Phys. Sin.* **60** 068102 (in Chinese)
[28] Zhao S C, Liu Z D, Zheng J and Li G 2011 *Chin. Phys.* B **20** 067802
[29] Zhao J, Chang B K, Xiong Y J and Zhang Y J 2011 *Chin. Phys.* B **20** 047801
[30] Wada S, Park S E, Cross L E and Shrout T R 1999 *Ferroelectrics* **221** 147
[31] Rajan K K, Shanthi M, Chang W S, Jin J and Lim L C 2007 *Sens. Actuators* A **133** 110
[32] He C J, Jing W P, Zhu K J and Qiu J H 2011 *IEEE Trans. Ultrason. Ferroelectr. Freq. Control* **58** 1118